# The Neutrophil Dynamic Mass Redistribution Assay as a Medium throughput Primary Cell Screening Assay [S]

Lisa A. Stott, Armand Drieu la Rochelle, Susan Brown, Greg Osborne, Catherine J. Hutchings, Simon Poulter, Kirstie A. Bennett, and Matt Barnes

*Sosei Heptares, Steinmetz Building, Granta Park, Cambridge, United Kingdom (L.A.S., A.D.R., S.B., G.O., S.P., K.A.B., M.B.); and Independent Consultant (C.J.H.)*

Received June 8, 2023; accepted September 12, 2023

## ABSTRACT

In a typical G protein coupled receptor drug discovery campaign, an in vitro primary functional screening assay is often established in a recombinant system overexpressing the target of interest, which offers advantages with respect to overall throughput and robustness of compound testing. Subsequently, compounds are then progressed into more physiologically relevant but lower throughput ex vivo primary cell assays and finally in vivo studies. Here we describe a dynamic mass redistribution (DMR) assay that has been developed in a format suitable to support medium throughput drug screening in primary human neutrophils. Neutrophils are known to express both CXC chemokine receptor (CXCR) 1 and CXCR2 that are thought to play significant roles in various inflammatory disorders and cancer. Using multiple relevant chemokine ligands and a range of selective and nonselective small and large molecule antagonists that block CXCR1 and CXCR2 responses, we demonstrate distinct pharmacological profiles in neutrophil DMR from those observed in recombinant assays but predictive of activity in neutrophil chemotaxis and CD11b upregulation, a validated target engagement marker previously used in clinical studies of CXCR2 antagonists. The primary human neutrophil DMR cell system is highly reproducible, robust, and less prone to donor variability observed in CD11b and chemotaxis assays and thus provides a unique, more physiologically relevant, and higher throughput assay to support drug discovery and translation to early clinical trials.

## SIGNIFICANCE STATEMENT

Neutrophil dynamic mass redistribution assays provide a higher throughput screening assay to profile compounds in primary cells earlier in the screening cascade enabling a higher level of confidence in progressing the development of compounds toward the clinic. This is particularly important for chemokine receptors where redundancy contributes to a lack of correlation between recombinant screening assays and primary cells, with the coexpression of related receptors confounding results.

## Introduction

The CXC chemokine receptor (CXCR) 2 is a G protein-coupled receptor (GPCR) that is widely expressed across immune cells (Cheng et al., 2019). Both CXCR2 and the closely related CXCR1 are $G\alpha_i$-coupled GPCRs that predominantly signal through inhibitory G proteins to reduce intracellular cAMP. Like many chemokine receptors, CXCR1 and CXCR2 are activated by multiple circulating chemokines, with CXCR1 activated by CXCL6 and CXCL8, whereas CXCR2 is activated by CXCL1, CXCL2, CXCL3, CXCL5, CXCL6, CXCL7, and CXCL8 (Ahuja and Murphy, 1996; Liu et al., 2016). This makes a CXCR2 screening cascade more complex than a single ligand-receptor system, with the ligand promiscuity of chemokine receptors often cited as a reason for the clinical failure of many chemokine-targeting therapies (Dyer, 2020).

As the most abundant leukocyte in circulation and a key regulator in disease processes, neutrophils are becoming an important pharmacological target (Németh et al., 2020). As such, detection of neutrophil activity in clinical studies has become increasingly significant, with CD11b upregulation now established as an important translational marker (Liston et al., 1998; Lazaar et al., 2011; Miller et al., 2015; Namour et al., 2016). CD11b is an integrin, which is upregulated in response to circulating chemoattractants, such as chemokines and complement proteins (Maas et al., 2018). CD11b binds to intracellular adhesion molecules 1 and 2 to mediate neutrophil

**ABBREVIATIONS:** CXCL, chemokine (CXC-motif) ligand; CXCR, chemokine (C-X-C motif) receptor; DMR, dynamic mass redistribution; fMLF, N-formylmethionyl-leucyl-phenylalanine; FPR, formyl peptide receptor; GPCR, G protein coupled receptor; PTx, pertussis toxin; RT, room temperature.

adhesion and migration through the endothelium to sites of infection (Maas et al., 2018). CD11b upregulation has been used as a target engagement marker in many clinical trials, including for the CXCR2 small molecule antagonists danirixin and SB-656933, where the latter used CD11b data to inform clinical doses (Liston et al., 1998; Lazaar et al., 2011; Miller et al., 2015; Namour et al., 2016). Other common neutrophil assays include superoxide production and chemotaxis. While technological advancements have improved the quality of these assays over the years, they are often low throughput and labor intensive, prone to assay variability, and highly susceptible to interdonor variability, making them unsuitable for more intensive screening (Gomez-Lopez et al., 2011; Silvestre-Roig et al., 2019).

Dynamic mass redistribution (DMR) assays are a label-free method to measure ligand responses. They are based on two alternative detection methods, namely light refraction and electrical impedance. Light-based methods involve optical biosensors that measure the change in the wavelength of refracted light upon cellular activation, whereas impedance methods measure the change in the impedance of current flow between two electrodes (Scott and Peters, 2010; Fang, 2011). While it is still unknown precisely what these readouts measure, they are thought to provide a holistic view of cellular signaling, detecting more integrated, phenotypic downstream responses, such as changes in cell adhesion or shape (Scott and Peters, 2010; Grundmann and Kostenis, 2015). Although most studies have examined recombinant cells in these systems, the high sensitivity and ability to capture any form of signaling in a label-free set-up affords an ideal opportunity for primary cell studies (Grundmann and Kostenis, 2015; Hillger et al., 2017). Moreover, the ability to pick up multiple signaling pathways and modalities makes them potentially superior to standard functional assays, which measure a single readout of response.

The unique expression of receptor and effector proteins in different cell backgrounds can dramatically change compound activity when transferring from recombinant systems, where primary pharmacology screening usually occurs, to endogenously expressing systems (Eglen et al., 2008). This is particularly true for chemokine receptors, where redundancy is thought be a major contributor to drug failures (Dyer, 2020), especially for neutrophils, which coexpress CXCR1 and CXCR2 (Futosi et al., 2013; Lämmermann and Kastenmüller, 2019). Thus, our objective was to establish a DMR assay to measure chemokine activation in primary human neutrophils and to determine how these results translate from data generated using recombinant cell systems. We also aimed to examine more conventional neutrophil assays (namely, CD11b upregulation and chemotaxis) to validate the DMR assay for higher throughput compound screening in primary cells. There is precedent for measuring GPCR activation in neutrophil DMR assays (Schröder et al., 2011; Locker et al., 2015; Christensen et al., 2017; Frei et al., 2021); however, to our knowledge, this is the first time a more thorough examination and comparison of multiple functional readouts for neutrophil chemokine receptors has been undertaken. As CD11b upregulation is a common target engagement marker for neutrophil GPCR drugs, we were keen to establish how results translate from the DMR platform to CD11b and whether this assay potentially could be used as a screen to help predict activity in a clinical setting. Here we demonstrate that neutrophil DMR assays are robust and reproducible, generating both chemokine responses and antagonist profiles that are consistent across different neutrophil assay formats, supporting DMR as a high-throughput alternative to CD11b and chemotaxis assays in the screening cascade.

## Materials and Methods

**Materials.** All chemokines were from Genscript (Piscataway, NJ, USA). All other ligands were from Tocris (Bristol, UK) except for AZD-5069 (MedChemExpress, Monmouth Junction, NJ, USA), Navarixin (Toronto Research Chemicals, Ontario, Canada), Danirixin (Cayman Chemical, Ann Arbor, MI, USA), N-formylmethionyl-leucyl-phenylalanine (fMLF) (Sigma Aldrich, Poole, UK), and human C5a (PeproTech, London, UK). Compound 19 (Dwyer et al., 2006) was synthesized internally. All assay reagents were from Sigma-Aldrich unless otherwise stated. FITC-conjugated mouse IgG1 kappa anti-CD11b monoclonal antibody (clone ICRF44, catalog no. 301330), APC-conjugated mouse IgGM kappa anti-CD15 monoclonal antibody (clone HI98, catalog no. 301908), and PE-Cy7-conjugated mouse IgG1 kappa anti-CD16 monoclonal antibody (clone 3G8, catalog no. 302016) were from Biolegend (San Diego, CA, USA) while CXCR2 nanobodies 127D1 and 163E3 (Bradley et al., 2015) were a kind gift from Kymab (Cambridge, UK).

**Cell Line Generation.** CHO-K1 cells were transfected with a pSNAP vector (NEB, Hitchin, UK) containing the human CXCR1 or CXCR2 receptor using GeneJuice transfection reagent (Merck Millipore, Watford, UK) according to the manufacturer's instructions. Cells were cultured in Dulbecco's modified Eagle's medium/Ham's F-12 medium supplemented with 10% fetal bovine serum and 1 mg ml$^{-1}$ geneticin for selection. Following 2 weeks of selection, cells were dilution cloned. Clonal CHO CXCR1 and CHO CXCR2 cells were maintained in Dulbecco's modified Eagle's medium/Ham's F-12 medium supplemented with 10% FBS and 0.2 mg ml$^{-1}$ geneticin to maintain selection pressure.

**cAMP Assays.** CHO CXCR1 and CHO CXCR2 cells were seeded overnight at 2000 and 1200 cells per well, respectively, in white 384-well plates. On experiment day, media was replaced with assay buffer (Hank's balanced salt solution; Lonza, Basel, Switzerland) supplemented with 20mM HEPES and 0.1% bovine serum albumin, pH 7.4) in the absence or presence of antagonists, for 1 hour at 37°C. Chemokines, in the presence of 1 $\mu$M forskolin, were added and plates further incubated for 5 minutes. cAMP was detected using cAMP Gi kit (Cisbio, Codolet, France) according to the kit instructions. Plates were read on a PHERAstar FS microplate reader (BMG LabTech, Offenburg, Germany) using standard homogeneous time resolved fluorescence settings. Homogeneous time resolved fluorescence ratios were determined by dividing emissions at 665 nm by emissions at 620 nm and multiplying by 10,000.

**Neutrophil Isolation–Ficoll-Dextran.** Human whole blood from healthy volunteers (Cambridge Bioscience, Cambridge, UK) was mixed 1:1 with 2% dextran in PBS to sediment the red blood cells. After 30 minutes, the supernatant was removed and carefully layered onto 15 ml Ficoll-Paque (GE Healthcare, Pittsburgh, PA, USA) and centrifuged for 25 minutes [300g, room temperature (RT), slow acceleration and brake]. The supernatant was discarded and the pellet resuspended in PBS. Contaminating red blood cells were removed by osmotic shock; 20 ml ice-cold distilled water was added for 30 seconds before neutralization with 20 ml 2x PBS. Cells were pelleted by centrifugation (5 minutes, 300g) before being resuspended in PBS. Cells were counted with a Haematology Analyzer (Sysmex, Milton Keynes, UK).

**Dynamic Mass Redistribution Assays.** Ficoll-Dextran isolated cells were resuspended in assay buffer containing 0.4% DMSO and seeded 50,000 neutrophils per well onto uncoated 384-well Epic plates (Corning, NY, USA). Cells were left to settle to the bottom of the wells at RT for 2 hours. Plates were read using the Corning Epic BT System, which measures cellular responses as a change in the wavelength of refracted light. First, plates were read for 1 minute to establish baseline before pausing the read. Ligands were added slowly and to

the top of the volume to avoid disturbing the cells, using a Bravo Automated Liquid Handling Platform (Agilent, Santa Clara, CA, USA). The plate was returned to the reader and the read resumed. For antagonist treatments, antagonists were added in the same manner with responses measured to determine the effect of compound alone. They were incubated for 1 hour at RT before the addition of chemokine as described earlier. For pertussis toxin (PTx) treatments, neutrophils were incubated with 3 $\mu$g ml$^{-1}$ PTx for 1 hour at 37°C before being plated onto Epic plates as stated previously. For CHO CXCR1 or CXCR2 assays, cells were seeded 12,500 cells per well overnight onto uncoated 384-well Epic plates. Media was exchanged for assay buffer for 2 hours prior to conducting assay as described earlier.

**Neutrophil Isolation–Magnetic Isolation.** Neutrophils were isolated from human whole blood from healthy volunteers by immunomagnetic negative selection using the EasySep Direct Human Neutrophil Isolation kit (STEMCELL Technologies, Cambridge, UK) following manufacturer's instructions. Briefly, EDTA was added to the blood to a final concentration of 1 mM before adding the isolation cocktail and Rapid-Spheres. After 5 minutes incubation at RT, the cells were diluted with 1 equal volume of PBS containing 1 mM EDTA and placed into the magnet for 10 minutes at RT to allow magnetic separation of labeled cells. Further enrichment was undertaken by performing two additional cycles of RapidSpheres addition and separation with the magnet. The final cell suspension was counted with a Haematology Analyzer with expected neutrophil purity > 90%. Cells were centrifuged (5 minutes, 300g) then resuspended in assay buffer.

**Chemotaxis Assays.** Magnetically isolated neutrophils were loaded with 5 $\mu$M Calcein AM (Invitrogen) for 30 minutes at 37°C before resuspension in assay buffer. Two hundred thousand cells were added to the upper chamber of a HTS 96-transwell chemotaxis plate with a 5 $\mu$m filter (Corning) and incubated for 30 minutes at 37°C in the presence or absence of antagonist. Following this incubation, chemokine was added to the lower well compartment and the filter plate assembly incubated at 37°C/5% CO$_2$ for 45 minutes. The filter was removed and 100 $\mu$l of the lower compartment was transferred to a 96-well black bottom plate (Corning) and the fluorescence determined (excitation: 485 nm emission: 520 nm) using a PHERAstar microplate reader.

**CD11b Assays.** Fifty thousand magnetically isolated human neutrophils were preincubated with antagonist at 37°C for 30 minutes before the addition of chemokine for 30 minutes at 37°C. The assay was stopped by placing cells on ice and addition of an equal volume of ice-cold staining buffer (1.5 $\mu$g ml$^{-1}$ anti-CD11b antibody + 0.4 $\mu$g ml$^{-1}$ anti-CD15 antibody + 0.1 $\mu$g ml$^{-1}$ anti-CD16 antibody in assay buffer). After staining for 30 minutes at 4°C, cells were washed twice with ice-cold assay buffer and fixed with 1% paraformaldehyde (20 minutes, 4°C). After fixation, cells were washed twice with ice-cold PBS and kept in 200 $\mu$l PBS at 4°C in the dark until ready to analyze. CD11b expression was determined using flow cytometry (FACS-Canto II; Becton, Dickinson and Company, Franklin Lakes, NJ, USA). Neutrophil CD11b expression was measured using the geometric mean of FITC fluorescence intensity on CD15-positive and CD16-positive granular cells with high forward and side-scatter properties; 2,000 positive events were counted per sample.

**Data Analysis.** DMR data were analyzed using Corning EpicAnalyzer software. Raw DMR traces were corrected by removal of background responses and the peak response between 3 and 7 minutes (neutrophil) or 5 and 12 minutes (CHO CXCR1 and CXCR2) extracted. All data were plotted in GraphPad Prism (San Diego, CA, USA) using four parameter logistic equation. Statistical analyses were also conducted with GraphPad Prism.

## Results

**Profiling of Chemokines and Antagonists in CHO CXCR1 and CHO CXCR2 cAMP and DMR Assays.** First, we profiled a range of chemokines and antagonists reported to be selective for CXCR1 and CXCR2 in CHO CXCR1 and

CXCR2 cAMP and DMR assays to understand their potencies and selectivity profiles in a recombinant expression system. As a G$\alpha_i$-coupled receptor, inhibition of cAMP is the primary signaling endpoint for CXCR1 and CXCR2, so we wanted to investigate how this compared with a DMR readout.

In the cAMP assay, all the chemokines examined were full agonists for the inhibition of forskolin-stimulated cAMP at the CXCR2 receptor, except for CXCL7 (E$_{max}$ 88 ± 3%; Table 1; Fig. 1A). At CXCR1, all ligands acted as full agonists to inhibit forskolin-stimulated cAMP, except for CXCL1, which was a partial agonist (E$_{max}$ 81 ± 6%) and CXCL2, which was inactive (Table 1; Fig. 1B). Between the two receptors, there were large potency differences for many of the chemokines tested, which is reflective of their reported variations in selectivity for CXCR2.

In the DMR assay, chemokines induced concentration-dependent positive deflections in both CHO CXCR2 (Fig. 1C) and CHO CXCR1 (Fig. 1D) cells, which peaked around 5 minutes after compound addition. Peak responses were extracted for both receptors (Fig. 1, E and F), with CXCR2 results appearing broadly consistent with the results of the cAMP assay (Table 1). However, there was a trend for reduced agonist potencies in this assay relative to the inhibition of cAMP, and CXCL2 was also identified as a partial agonist. This is likely due to the increased signal amplification of the cAMP signal, leading to increased agonist potencies (Stott et al., 2016). However, the correlation in potencies between both assay formats for CXCR2 was poor (R$^2$ = 0.27; Fig. 1G), though this is potentially due to the low spread in potency values across ligands at this target and the higher variability in the DMR responses. For CXCR1, the DMR readout revealed the partiality of most of the chemokines at this target, with only the two CXCL8 proteoforms showing full agonism (Fig. 1F; Table 1). Unlike CXCR2, there was an excellent correlation in potencies for CXCR1 between the two assay formats (R$^2$ = 0.92; Fig. 1H) as well as a trend for increased potencies in DMR relative to cAMP, opposite to what was observed for CXCR2.

We then tested a range of small molecule antagonists, most of which have been previously described as CXCR2-selective, in the CHO CXCR1 and CXCR2 cAMP and DMR assays using both CXCL8 and CXCL1 as nonselective and selective chemokines, respectively (Fig. 2). Due to the weak activity of CXCL1 at CXCR1, we could not determine the activity of the antagonists for this receptor-ligand pair. All the small molecules tested were able to fully inhibit CXCR2 responses elicited by both CXCL8 and CXCL1, except for reparixin, which was inactive, and NVP CXCR2 20, which partially inhibited the CXCR2 responses (Fig. 2, A and B; Table 2). Reparixin is described as a high-affinity antagonist of both CXCR1 and CXCR2 (Bertini et al., 2004), so this inactivity was surprising. We cannot yet explain this contradictory observation; we tested multiple sources of the compound and quality control analysis by UV, and mass spectrometry (data not shown) did not highlight any issues with the compound stock. There were no significant differences in the potencies of the small molecules to inhibit CXCR2 signaling induced by CXCL1 or CXCL8 (P > 0.05; unpaired t test), but all ligands were significantly less potent at inhibiting CXCL8 signaling at CXCR1 when compared with CXCR2 (P < 0.05; unpaired t test; Fig. 2C; Table 2). We also examined two previously described CXCR2 specific nanobodies (Bradley et al., 2015). These nanobodies have been shown to either bind the CXCR2 N-terminus (clone 127D1), generating a potent, partial antagonist, or the extracellular loop (clone 163E3),

TABLE 1
Summary of chemokine responses in CHO CXCR2 and CXCR1 cAMP inhibition and DMR assays

| | CXCR2 | | | | CXCR1 | | | | |
|---|---|---|---|---|---|---|---|---|---|
| | cAMP[a] | | DMR[b] | | cAMP[a] | | DMR[b] | | Selectivity over CXCR1 (cAMP) |
| | $pEC_{50}$ | Max Response (% 6.3 nM CXCL8) | $pEC_{50}$ | Max Response (% 10 nM CXCL8) | $pEC_{50}$ | Max Response (% 20 nM CXCL8) | $pEC_{50}$ | Max Response (% 10 nM CXCL8) | |
| CXCL1 | 9.89 ± 0.18 | 101 ± 7 | 9.06 ± 0.30 | 110 ± 21 | 7.21 ± 0.11 | 81 ± 6 | 8.48 ± 0.00 | 24 ± 0 | 460 |
| CXCL2 | 9.44 ± 0.22 | 99 ± 8 | 9.25 ± 0.15 | 59 ± 4 | ND | ND | ND | ND | >1,000 |
| CXCL3 | 9.84 ± 0.11 | 108 ± 5 | 9.15 ± 0.06 | 89 ± 9 | 6.88 ± 0.08 | 100[c] | ND | ND | 1264 |
| CXCL5 | 9.56 ± 0.23 | 103 ± 7 | 9.32 ± 0.32 | 90 ± 6 | 7.46 ± 0.08 | 97 ± 3 | 8.39 ± 0.64 | 27 ± 1 | 121 |
| CXCL5 (5-78) | 9.61 ± 0.18 | 108 ± 4 | 8.98 ± 0.28 | 86 ± 13 | 7.34 ± 0.08 | 102 ± 5 | 8.33 ± 0.00 | 11 ± 7 | 189 |
| CXCL5 (9-78) | 10.64 ± 0.19 | 103 ± 5 | 9.17 ± 0.19 | 104 ± 7 | 8.62 ± 0.12 | 97 ± 5 | 8.76 ± 0.18 | 78 ± 3 | 98 |
| CXCL6 | 8.80 ± 0.04 | 105 ± 2 | 8.53 ± 0.08 | 88 ± 2 | 7.71 ± 0.13 | 99 ± 7 | 8.20 ± 0.17 | 70 ± 14 | 11 |
| CXCL7 | 10.54 ± 0.20 | 88 ± 3 | 9.37 ± 0.33 | 69 ± 4 | 8.03 ± 0.17 | 97 ± 7 | 8.32 ± 0.04 | 38 ± 1 | 280 |
| CXCL8 | 10.10 ± 0.16 | 102 ± 1 | 9.73 ± 0.20 | 98 ± 3 | 9.72 ± 0.07 | 99 ± 4 | 9.61 ± 0.04 | 99 ± 3 | 2 |
| CXCL8 (8-79) | 10.07 ± 0.15 | 111 ± 5 | 8.78 ± 0.39 | 116 ± 12 | 9.75 ± 0.12 | 99 ± 6 | 9.42 ± 0.04 | 91 ± 5 | 2 |

ND, not determined due to no/little activity up to 200nM.
[a]All cAMP data are pooled (mean ± S.D.) of four to five independent experiments performed in triplicate.
[b]All DMR data are pooled (mean ± S.D.) of two to four independent experiments performed in duplicate.
[c]CXCL3 maximal responses constrained to 100% to derive $pEC_{50}$ values due to incomplete curves.

generating a less potent but full antagonist (Bradley et al., 2015). In our hands, both nanobodies behaved as full antagonists, and, unlike the original report, 127D1 and 163E3 were equipotent at inhibiting both CXCL1 and CXCL8 responses (Table 2). These nanobodies have been shown not to bind CXCR1 (Bradley et al., 2015). When these antagonists were tested in the DMR assay, all ligands except reparixin and AZ 10397767 fully inhibited chemokine responses and the same rank order of $pIC_{50}$ values was obtained (Fig. 2, D–F; Table 3), and there was a good correlation with the cAMP results ($R^2 \geq 0.67$; Fig. 2, G–I). However, this assay had a much smaller assay window and much greater variability than the cAMP format, which limited compound testing.

**Chemokines Generate Robust and Reproducible DMR Responses That Are Specific to CXCR1 and CXCR2 in Isolated Neutrophils.** We then looked to characterize the chemokine and antagonist responses in the neutrophil DMR assay. While there is some evidence for CXCL8-induced neutrophil DMR responses (Locker et al., 2015), this is the first time a more detailed assessment of chemokine responses in this assay, and how they compare with other neutrophil assays, has been undertaken. Upon addition of chemokine, neutrophils demonstrated a large and rapid concentration-dependent positive deflection which peaked within 4 minutes of treatment (Fig. 3, A–C), which was much larger in size than the CHO CXCR1 or CHO CXCR2 DMR assays (Fig. 1, C and D). All chemokines displayed very similar kinetic traces, despite the differing levels of selectivity for CXCR2 over CXCR1 (Table 1). Peak responses were extracted and data pooled (Fig. 3, D and E) with chemokine potencies and maximal responses described in Table 4. Despite the known issues of reproducibility in primary cell assays, ligand potencies were very consistent over multiple donors, although absolute response magnitude varied; for example, 30 nM CXCL8 responses ranged from ~700 to 1200 Δpm between donors, but intra-assay variability was generally less than 10% (Supplemental Fig. 1) and
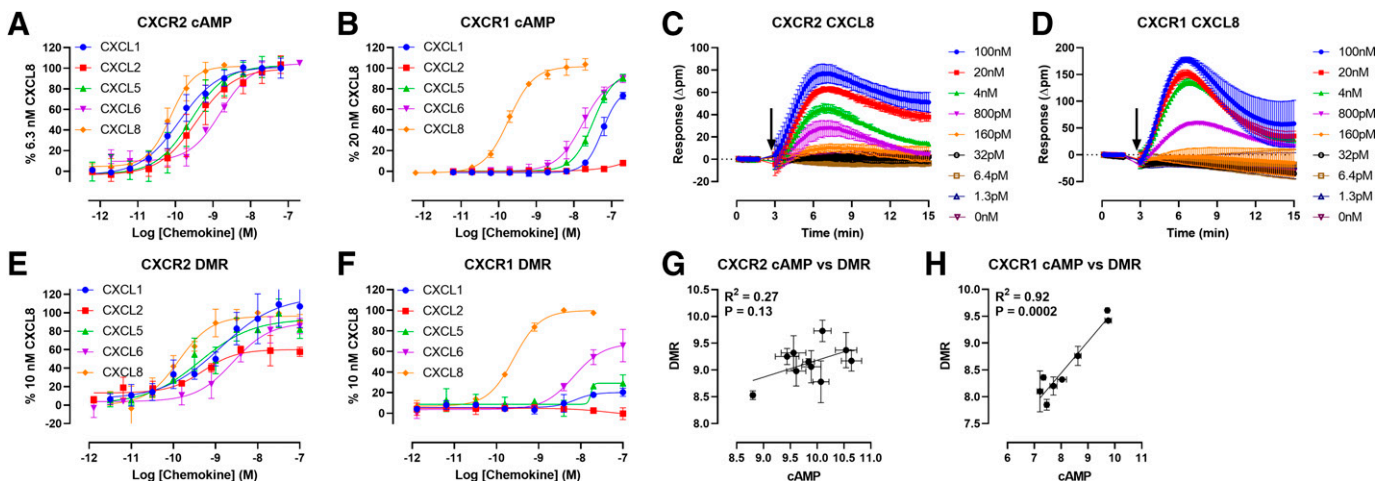


**Fig. 1.** Activity of chemokine ligands in CHO CXCR1 and CHO CXCR2 cAMP and DMR assays. Example chemokine concentration response curves for cAMP assays in CHO CXCR2 (A) and CXCR1 (B) assays. Representative kinetic DMR traces for CXCL8 at CXCR2 (C) and CXCR1 (D) with compound addition indicated by the arrow. Example chemokine concentration response curves for DMR assays for CXCR2 (E) and CXCR1 (F). There was a poor correlation in potencies between the two readouts for CXCR2 (G) but an excellent correlation for CXCR1 (H). Data are pooled (mean ± S.D.) from two to five independent experiments with data in correlation plots summarized from Table 1. For the kinetic traces, data are mean ± S.D. from duplicate wells.
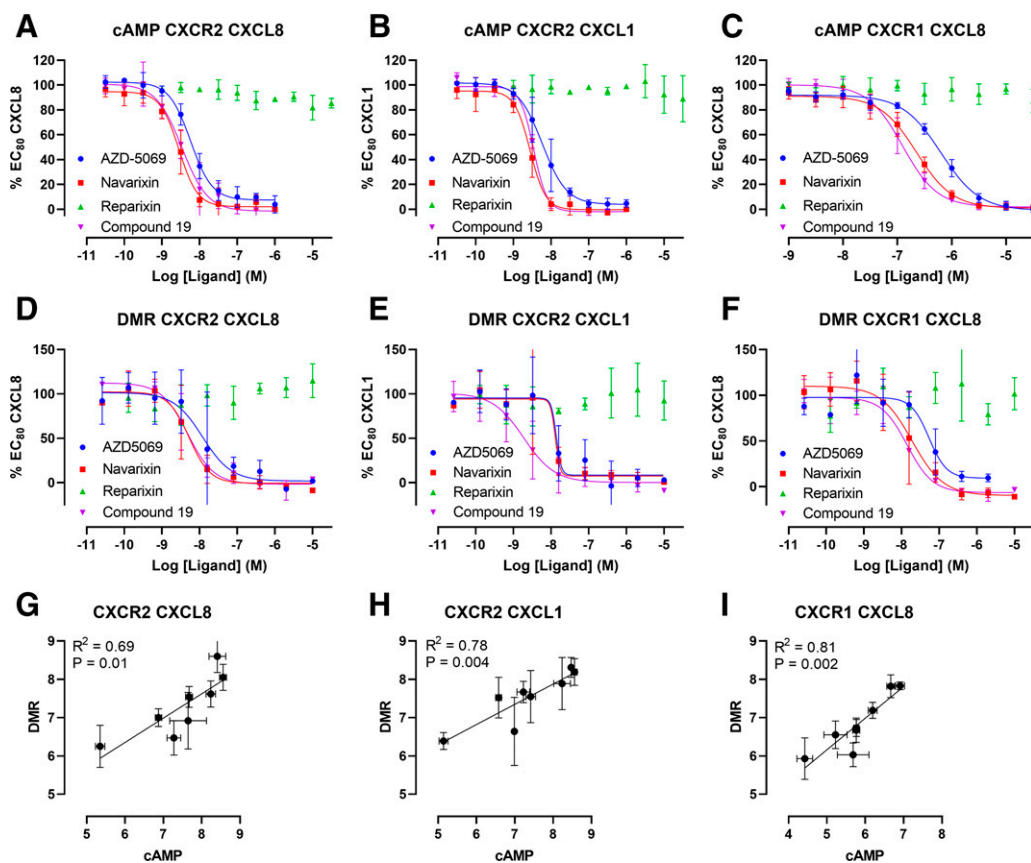
**Fig. 2.** Activity of antagonists in CHO CXCR1 and CHO CXCR2 cAMP and DMR assays. Antagonists were preincubated with for 1 hour at RT prior to addition of EC$_{80}$ of chemokine. Example antagonist concentration response curves at CXCR2 (A, B) and CXCR1 (C) in cAMP assays and CXCR2 (D, E) and CXCR1 (F) in DMR assays. pIC$_{50}$s between assay formats correlated well (G–I). All data are pooled (mean ± S.D.) of two to four experiments with data in correlation plots summarized from Table 2.

much lower than that previously reported for formyl peptide receptor (FPR) 1 responses in the same assay (Christensen et al., 2017).

We then compared the chemokine potencies in neutrophil DMR with those from CHO CXCR2 cAMP and observed a good correlation between the two assays ($R^2$ = 0.63, $P$ < 0.01; Fig. 3F). However, the correlation between CHO CXCR2 DMR and neutrophil DMR was much lower ($R^2$ = 0.32, $P$ = 0.09; Fig. 3G). Compared with the neutrophil DMR, the CHO CXCR2 DMR had a much lower signal (∼100 pM vs ∼1000 pM) and much greater variability. This could be reflective of different

cellular processes within the different cell backgrounds upon CXCR2 activation, which could explain these results. When the neutrophil DMR potencies were compared with the CHO CXCR1 cAMP results, there was no correlation ($R^2$ = 0.00; data not shown), likely due to the selectivity of most chemokines for CXCR2.

As DMR likely represents a holistic cellular response, we wanted to investigate whether the chemokine responses measured in neutrophils were dependent on G$\alpha_i$ activation using PTx to inactivate the G$\alpha_i$ protein. However, neutrophils are short-lived cells that usually only survive for less than 24 hours

TABLE 2
Summary of antagonist responses at CHO CXCR2 and CXCR1 receptors in cAMP inhibition assays against an EC$_{80}$ challenge of CXCL1 and CXCL8

| | CXCR2 | | | | CXCR1 | | |
|---|---|---|---|---|---|---|---|
| | CXCL1 | | CXCL8 | | CXCL8 | | |
| Compound | pIC$_{50}$ | % Inhibition | pIC$_{50}$ | % Inhibition | pIC$_{50}$ | % Inhibition | Selectivity over CXCR1 |
| AZD-5069 | 8.23 ± 0.22 | 95 ± 1 | 8.24 ± 0.12 | 93 ± 5 | 6.19 ± 0.12 | 101 ± 3 | 110 |
| Navarixin | 8.58 ± 0.09 | 100 ± 4 | 8.56 ± 0.09 | 97 ± 1 | 6.66 ± 0.10 | 99 ± 1 | 78 |
| Reparixin | IA | IA | IA | IA | IA | IA | — |
| Danirixin | 7.42 ± 0.13 | 91 ± 7 | 7.67 ± 0.09 | 94 ± 4 | 5.77 ± 0.07 | 99 ± 2 | 80 |
| AZ 10397767 | 7.23 ± 0.18 | 106 ± 8 | 7.66 ± 0.49 | 104 ± 1 | 5.68 ± 0.41 | 104 ± 2 | 91 |
| Compound 19 | 8.47 ± 0.03 | 102 ± 3 | 8.40 ± 0.22 | 105 ± 7 | 6.91 ± 0.12 | 98 ± 1 | 32 |
| SB 225002 | 6.58 ± 0.08 | 101 ± 4 | 6.88 ± 0.09 | 98 ± 5 | 5.22 ± 0.30 | 67 ± 31 | 45 |
| NVP CXCR2 20 | 5.14 ± 0.12 | 77 ± 19 | 5.42 ± 0.06 | 82 ± 5 | 4.42 ± 0.20 | 97 ± 18 | 9 |
| SB 265610 | 6.99 ± 0.02 | 106 ± 3 | 7.27 ± 0.18 | 101 ± 3 | 5.76 ± 0.09 | 94 ± 0 | 32 |
| 127D1 | 8.39 ± 0.12 | 97 ± 8 | 8.33 ± 0.23 | 87 ± 15 | NT | NT | — |
| 163E3 | 8.35 ± 0.05 | 103 ± 5 | 8.31 ± 0.07 | 101 ± 6 | NT | NT | — |

IA, inactive; NT, not tested.
Data are pooled (mean ± S.D.) from at least three independent experiments performed in duplicate. % inhibition is expressed as a percentage of the 10 $\mu$M navarixin response. CXCL1 antagonism at CXCL8 could not be determined due to low activity of CXCL1 at this receptor, so CXCR2 selectivity over CXCR1 was calculated from pIC$_{50}$s from CXCL8 inhibition at each receptor in cAMP assays.

TABLE 3
Summary of antagonist responses at recombinant CHO CXCR2 and CXCR1 receptors in DMR assays against an EC$_{80}$ challenge of CXCL1 and CXCL8

| | CXCR2 | | | | CXCR1 | |
| | CXCL1 | | CXCL8 | | CXCL8 | |
| Compound | pIC$_{50}$ | % Inhibition | pIC$_{50}$ | % Inhibition | pIC$_{50}$ | % Inhibition |
|---|---|---|---|---|---|---|
| AZD-5069 | 7.89 ± 0.68 | 101 ± 5 | 7.62 ± 0.34 | 97 ± 4 | 7.19 ± 0.21 | 89 ± 3 |
| Navarixin | 8.19 ± 0.35 | 100 ± 3 | 8.05 ± 0.34 | 92 ± 5 | 7.82 ± 0.30 | 103 ± 7 |
| Reparixin | IA | IA | IA | IA | IA | IA |
| Danirixin | 7.55 ± 0.68 | 100 ± 5 | 7.54 ± 0.27 | 104 ± 2 | 6.73 ± 0.22 | 94 ± 11 |
| AZ 10397767 | 7.68 ± 0.23 | 52 ± 24 | 6.28 ± 1.08 | 99 ± 8 | 6.03 ± 0.31 | 62 ± 12 |
| Compound 19 | 8.31 ± 0.26 | 99 ± 4 | 8.60 ± 0.42 | 98 ± 7 | 7.83 ± 0.10 | 102 ± 7 |
| SB 225002 | 7.52 ± 0.53 | 92 ± 12 | 7.00 ± 0.23 | 91 ± 7 | 6.55 ± 0.36 | 82 ± 18 |
| NVP CXCR2 20 | 6.39 ± 0.22 | 79 ± 30 | 6.25 ± 0.55 | 93 ± 7 | 5.93 ± 0.54 | 103 ± 7 |
| SB 265610 | 6.64 ± 0.89 | 90 ± 21 | 6.47 ± 0.45 | 98 ± 8 | 6.67 ± 0.32 | 95 ± 8 |

IA, inactive.
Data are pooled (mean ± S.D.) from two to four independent experiments performed in duplicate. % inhibition is expressed as a percentage of the 10 $\mu$M navarixin response.

in the bloodstream (McCracken and Allen, 2014); this prohibited the usual overnight PTx treatment regimen. Instead, we used a modified protocol from Christensen et al. (Christensen et al., 2017) whereby we treated neutrophils for 1 hour with a high PTx concentration (3 $\mu$g ml$^{-1}$) and included fMLF as a positive control to replicate that study. However, this treatment only inhibited responses by around 20% (Supplemental Fig. 2) unlike the original study, which could inhibit responses by around 70%. In both cases, this suggests that there is some involvement of G$\alpha_i$ in the neutrophil DMR responses, but it likely needs a longer treatment time to fully inactivate the G$\alpha_i$ proteins, which is challenging to do with such short-lived cells.

As neutrophils express several GPCRs, we wanted to confirm that the responses detected were specific to CXCR1 and CXCR2. The chemokines show differing levels of selectivity for CXCR1 and CXCR2; therefore, we examined antagonism of both CXCL1 and CXCL8 as CXCR2-selective and -nonselective chemokines, respectively. It is noteworthy that most of the small molecules studied, except for the inactive reparixin,

induced a small, negative deflection following compound treatment alone (Fig. 4, A–C). This could be indicative of inverse agonism, which is generally characterized by an opposite response to the agonist. It has been demonstrated previously in DMR assays (Scott and Peters, 2010), and inverse agonism has been reported for both small molecule and nanobody CXCR2 antagonists (Bradley et al., 2009, 2015) but only in recombinant systems thus far. However, the scale of this response ($\sim$40 $\Delta$pm) is dwarfed by the response elicited by the chemokines themselves. These negative deflections were not observed in the CHO CXCR1 or CXCR2 DMR assays, suggesting the presence of constitutively active receptors in neutrophils that were not detected recombinantly. However, this could be due to the relative size responses between cell types; the assay signal in the recombinant system may not have been large enough to detect the constitutive activity. Notably, the nanobody 127D1 displayed a significant response when tested alone at concentrations of 3 nM and greater, suggesting either agonism or nonspecific responses at these higher concentrations. This effect was not observed for 163E3, suggesting it
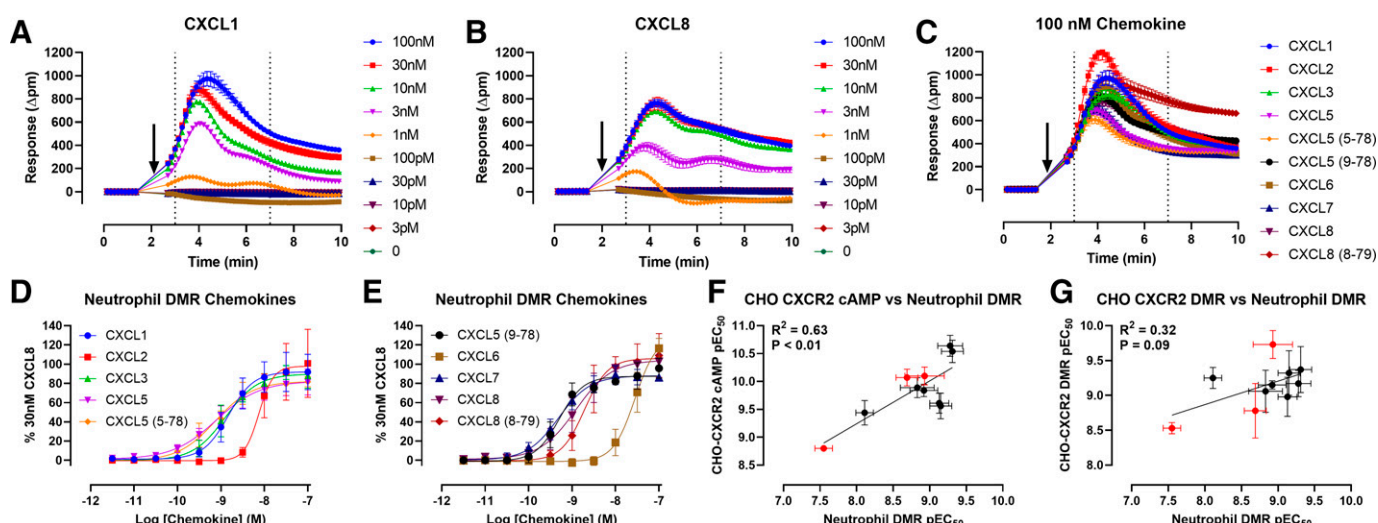


**Fig. 3.** CXCR1/2 chemokines demonstrate large positive deflections in neutrophil DMR assays. Representative kinetic DMR traces of concentration response curves of CXCL1 (A) and CXCL8 (B) and representative 100 nM chemokine (C) with arrow indicating compound addition. Data are mean ± S.D. of triplicate wells. Data were baseline corrected by subtracting buffer wells and peak response between 3 and 7 minutes extracted and plotted (D, E). Data represent pooled (mean ± S.D.) of at least four independent experiments each from an individual donor, normalized to 30 nM CXCL8 response. Neutrophil DMR potencies were correlated with potencies from recombinant CHO-CXCR2 cAMP (F) and DMR (G) with CXCR1/2 dual chemokines (CXCL6 and CXCL8) labeled in red.

TABLE 4
Summary of chemokine responses in neutrophil DMR assays

| Chemokine | $pEC_{50}$ | $E_{max}$ (% 30 nM CXCL8) | n |
|---|---|---|---|
| CXCL1 | 8.83 ± 0.23 | 92 ± 17 | 9 |
| CXCL2 | 8.11 ± 0.13 | 100 ± 29 | 4 |
| CXCL3 | 8.92 ± 0.13 | 90 ± 7 | 4 |
| CXCL5 | 9.15 ± 0.22 | 80 ± 12 | 9 |
| CXCL5 (5-78) | 9.13 ± 0.13 | 82 ± 8 | 4 |
| CXCL5 (9-78) | 9.28 ± 0.17 | 88 ± 8 | 4 |
| CXCL6 | 7.55 ± 0.12 | 129 ± 7 | 4 |
| CXCL7 | 9.31 ± 0.15 | 88 ± 2 | 4 |
| CXCL8 | 8.93 ± 0.27 | 104 ± 4 | 9 |
| CXCL8 (8-79) | 8.69 ± 0.15 | 106 ± 16 | 4 |

Data are expressed as pooled (mean ± S.D.) of at least four independent experiments from at least four individual donors, with maximal responses normalized to 30 nM CXCL8 response.

was not a general nonspecific effect to nanobody treatment (Fig. 4, D and E). These concentrations were excluded from further analysis. These agonist-like responses were also not observed in the CHO CXCR2 cells and could be due to off-target effects specific to neutrophils. This further emphasizes the need for primary cell screening in the target cell type.

All the small molecules examined inhibited both CXCL1- and CXCL8-induced DMR responses in a concentration-dependent manner, except for reparixin, which was inactive, in line with the recombinant data. When the CXCR2 nanobodies were examined, they showed significant inhibition of the CXCL1 response, but, unlike the recombinant assay data, 127D1 was 10-fold more potent than 163E3 and demonstrated partial antagonism. This is consistent with a previous report of the nanobody pharmacology (Bradley et al., 2015). However, when they were tested against CXCL8, they failed to significantly inhibit responses and potencies could not be derived due to incomplete curves (Fig. 5, A–F; Table 5). When the $pIC_{50}$ values for CXCR1 inhibition were compared between the neutrophil DMR assay and the CHO CXCR2 cAMP or DMR assays, there was an excellent correlation ($R^2$ = 0.73–0.74; Fig. 5, G and H). In contrast, the correlation for CXCL8 inhibition between neutrophil DMR and recombinant assays was lower for the DMR assay ($R^2$ = 0.65) and failed to reach significance for the cAMP assay ($R^2$ = 0.46;

$P$ = 0.06) (Fig. 5, I and J). CXCL1 displays one of the highest selectivities for CXCR2 (Table 1), so it is highly probable that at $EC_{80}$ concentration, only CXCR2 receptors are being activated, whereas CXCL8 will activate both CXCR1 and CXCR2. The reduced correlation for CXCL8 is likely indicative of two receptors signaling in neutrophils, compared with the single receptor system measured in the CHO CXCR1 and CXCR2 cell lines.

**Neutrophil DMR Assays Are Sensitive to Different Antagonist Modalities.** Next, we wanted to explore whether this assay was sensitive enough to pick up different antagonist modalities by performing Schild analysis using the CXCR2 nanobodies that have been described as noncompetitive (127D1) or competitive (163E3) (Bradley et al., 2015). We also compared these to AZD-5069, a slowly dissociating reversible small molecule antagonist (Nicholls et al., 2015) that may bind to an intracellular binding site previously identified for other CXCR2 small molecules (Bradley et al., 2009; Salchow et al., 2010; Liu et al., 2020). As shown in Fig. 6, all antagonists generated different profiles at CXCL1 that were broadly consistent with their reported pharmacological profiles. The N-terminal binder 127D1 acted as a negative allosteric modulator, where increasing concentrations of antagonist could no longer compete with the agonist due to co-operativity, leading to characteristic "stacking" of the agonist curves (Fig. 6A). However, the reported competitive binder 163E3 caused a decrease in the maximal response and did not show the competitive antagonist profile previously reported (Fig. 6B). The small molecule AZD-5069 also caused a decrease in the maximal response of CXCL1, appearing as a noncompetitive antagonist (Fig. 6C), which is likely due to its previously reported slow dissociation rate. This contrasts with the responses observed at CXCL8, where only AZD-5069 and 300 nM 163E3 showed any significant inhibition of the CXCL8 response (Fig. 6, D–F). Furthermore, unlike the CXCL1 inhibition, AZD-5069 failed to fully inhibit CXCL8 responses at 1 $\mu$M and much higher concentrations of compound are required to fully block the signaling of this chemokine. As none of these antagonists show competitive profiles, we could not determine a $pA_2$ for any of the compounds.
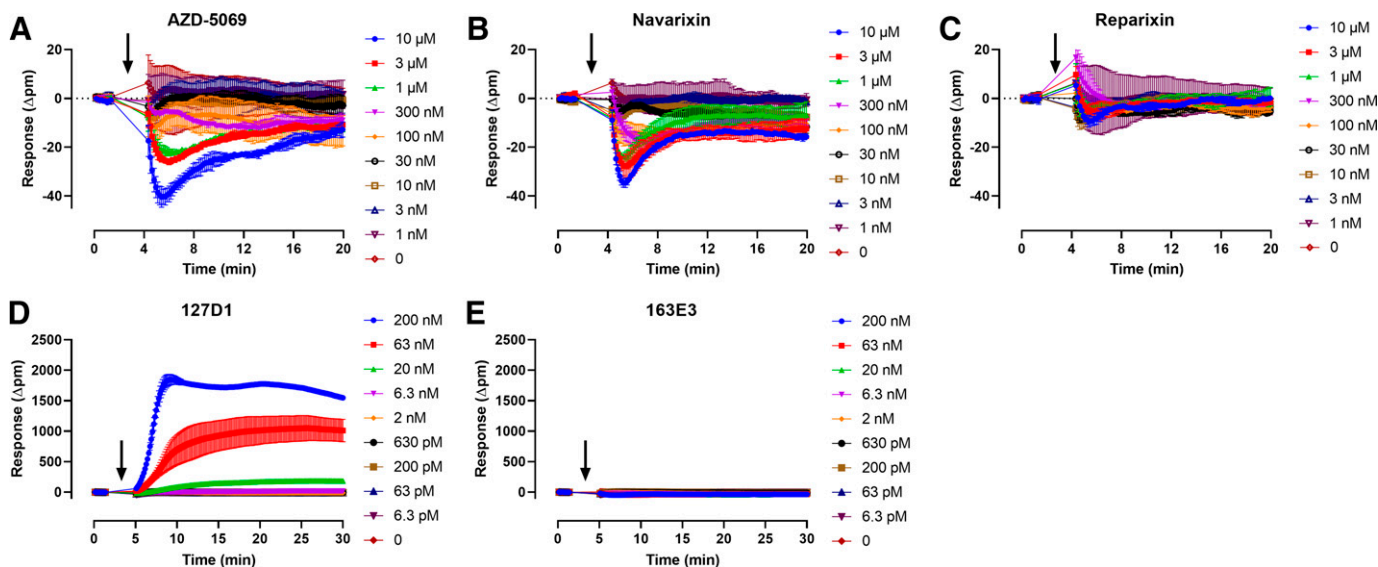


**Fig. 4.** Kinetic traces of antagonist treatments. Representative kinetic DMR traces of small molecule antagonist (A–C) and nanobody treatments (D, E). Data represents mean ± S.D. of duplicate wells with arrow indicating compound addition.
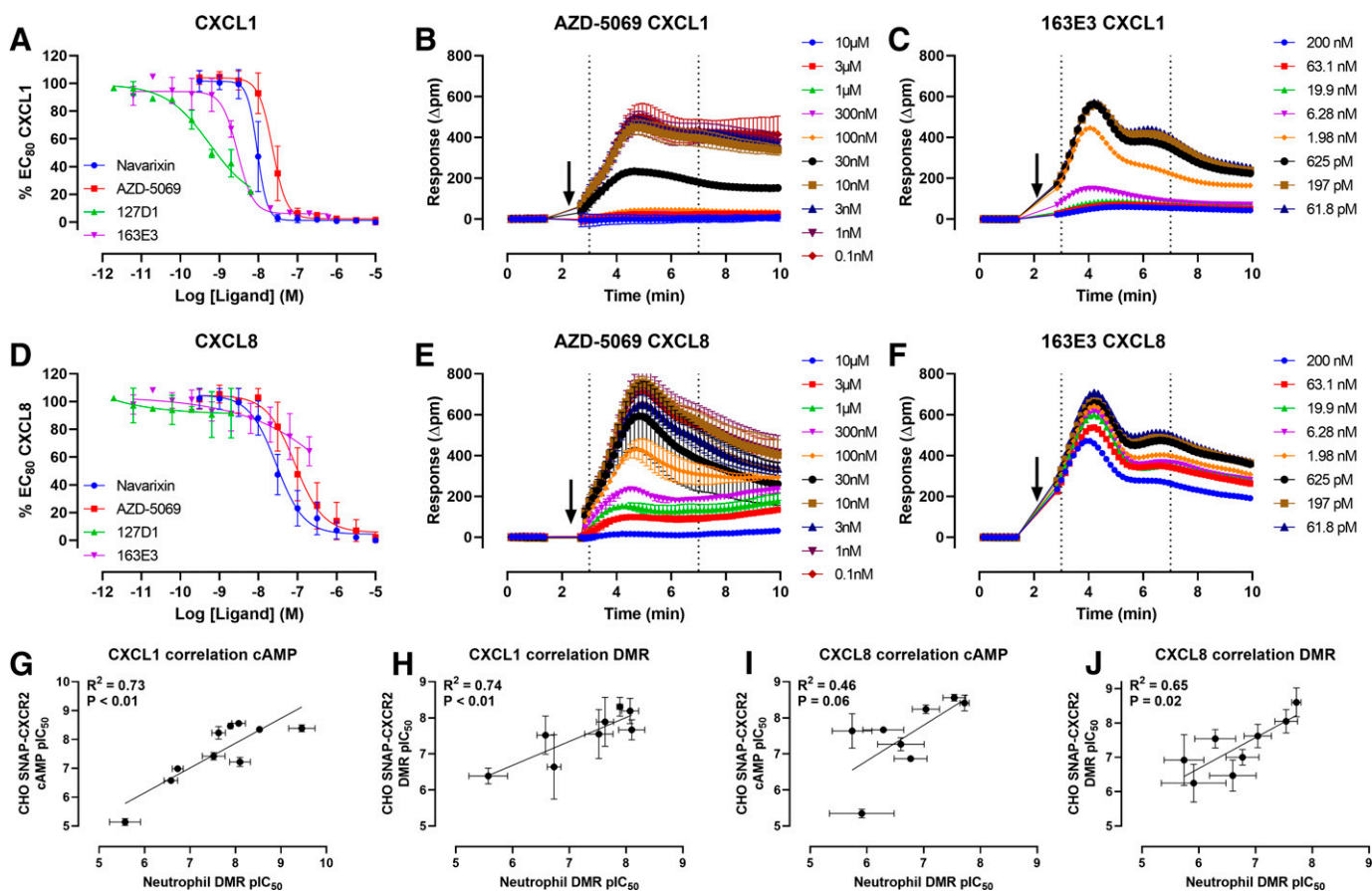
**Fig. 5.** Inhibition of CXCL1 and CXCL8 responses by CXCR1/2 antagonists. Antagonists were preincubated with neutrophils for 1 hour at RT prior to addition of $EC_{80}$ of chemokine. Inhibition of CXCL1 (A) and CXCL8 (D) induced DMR responses by selected antagonists. Data are pooled (mean ± S.D.) of 4 to 15 independent experiments, each from an individual donor, performed in duplicate, normalized to $EC_{80}$ concentration of chemokine. Representative DMR kinetic traces of $EC_{80}$ chemokine addition following preincubation with increasing concentration of AZD-5069 (B, E) or 163E3 (C, F). Data points represent mean ± S.D. of duplicate wells. Correlation between $pIC_{50}$ for neutrophil DMR and CHO CXCR2 CXCL1 cAMP (G), CXCL1 DMR (H), CXCL8 cAMP (I), or CXCL8 DMR (J).

**Neutrophil DMR Assays Yield Comparable Results to Traditional CD11b and Chemotaxis Assays.** We have demonstrated that a DMR approach can be successfully applied to neutrophils to investigate chemokine pharmacology and provide robust and reproducible data. Given the holistic nature of the DMR signal, we aimed to confirm our observations in well-established assays. To support this, we assessed the upregulation of the CD11b integrin by flow cytometry, a standard readout validated as a target engagement marker in neutrophils (Liston et al., 1998; Lazaar et al., 2011; Miller et al., 2015; Namour et al., 2016), and we used the low throughput, but more mechanistic, in vitro chemotaxis assay. All chemokines examined induced concentration-dependent upregulation of CD11b with results broadly complimenting those from the DMR assay (Fig. 7, A and B; Table 6); however, in contrast to the DMR assay, both the CD11b and chemotaxis assays show much greater donor to donor variability (Supplemental Fig. 3). This variability for the chemotaxis assays particularly meant we could test fewer antagonists in this assay. It also precluded the determination of an $EC_{80}$ and prohibited standard $IC_{50}$ determination in this assay format. A further advantage of the DMR assay is the lack of "bell-shaped" response that is characteristic of the chemotaxis assay.

When challenged against an $EC_{80}$ concentration of CXCL1, AZD-5069, 127D1, and 163E3 all inhibited responses with

$pIC_{50}$s of 8.19 ± 0.19, 9.55 ± 0.24, and 8.30 ± 0.26, respectively, which were consistent with their $pIC_{50}$s in the DMR assay (Fig. 7C). However, AZD-5069 was the only antagonist to inhibit CXCL8 responses in the CD11b assay (Fig. 7D), and its potency was 69-fold lower at 6.53 ± 0.10. This is consistent with the DMR data and further supports that both CXCR1 and CXCR2 are involved in neutrophil chemokine responses. We also wanted to reproduce the Schild neutrophil DMR experiments to determine whether the noncompetitive profiles of the antagonists tested would also be mirrored in both CD11b and chemotaxis assays.

While the lower throughput of the chemotaxis prevented us from testing a wider range of antagonist concentrations, both assay formats agreed with the negative allosteric modulator profile of 127D1 and the reduction in maximal response with 163E3 when tested against CXCL1 responses (Fig. 7, E–H). In contrast, neither nanobody could block CXCL8 responses in either the CD11b or chemotaxis assays (Fig. 7, I–L). Furthermore, AZD-5069 demonstrated inhibitory profiles consistent with the DMR responses in CD11b, with noncompetitive inhibition of CXCL1 and increased concentrations required to fully inhibit CXCL8 (Fig. 7, M and N).

**Neutrophil DMR Assays Can Be Applied to a Range of GPCRs.** Finally, following the success of neutrophil DMR assays for detecting CXCR1 and CXCR2 responses, we investigated the

TABLE 5
Summary of CXCL1 and CXCL8 inhibition by antagonists in neutrophil DMR assays

| | CXCL1 | | | CXCL8 | | | | |
|---|---|---|---|---|---|---|---|---|
| | $pIC_{50}$ | Max Inhibition | Hill Slope | $pIC_{50}$ | Max Inhibition | Hill Slope | n | Selectivity over CXCR1[a] |
| AZD-5069 | 7.63 ± 0.15 | 97 ± 2 | 3.22 ± 1.11 | 7.04 ± 0.24 | 96 ± 5 | 1.34 ± 0.50 | 15 | 110 |
| Navarixin | 8.07 ± 0.15 | 99 ± 1 | 3.59 ± 1.05 | 7.54 ± 0.20 | 97 ± 4 | 1.33 ± 0.39 | 15 | 78 |
| Reparixin | IA | IA | IA | IA | IA | IA | 5 | — |
| Danirixin | 7.52 ± 0.25 | 99 ± 4 | 0.68 ± 0.23 | 6.29 ± 0.36 | 101 ± 3 | 0.76 ± 0.11 | 4 | 80 |
| AZ 10397767 | 8.10 ± 0.23 | 96 ± 2 | 0.76 ± 0.38 | 5.74 ± 0.35 | 95 ± 10 | 0.65 ± 0.11 | 4 | 91 |
| Compound 19 | 7.89 ± 0.05 | 102 ± 2 | 4.28 ± 0.53 | 7.72 ± 0.08 | 96 ± 3 | 2.98 ± 0.57 | 4 | 32 |
| SB 225002 | 6.58 ± 0.15 | 92 ± 14 | 0.82 ± 0.26 | 6.77 ± 0.29 | 74 ± 18 | 1.38 ± 0.63 | 4 | 45 |
| NVP CXCR2 20 | 5.57 ± 0.34 | 86 ± 19 | 1.13 ± 0.97 | 5.91 ± 0.57 | 86 ± 17 | 0.84 ± 0.31 | 5 | 9 |
| SB 265610 | 6.73 ± 0.12 | 101 ± 3 | 0.59 ± 0.18 | 6.60 ± 0.41 | 99 ± 6 | 0.69 ± 0.20 | 4 | 32 |
| 127D1 | 9.46 ± 0.29 | 73 ± 15 | 1.23 ± 0.35 | IA | IA | IA | 4 | — |
| 163E3 | 8.53 ± 0.03 | 94 ± 1 | 2.11 ± 0.26 | ND | ND | ND | 4 | — |

IA, inactive; ND, not determined due to incomplete curve.
[a]Antagonist selectivity for CXCR2 over CXCR1 was determined from inhibition of $EC_{80}$ concentration of CXCL8 in recombinant cells (Table 2).
Data are pooled (mean ± S.D.) of at least four independent experiments performed in duplicate, with maximal inhibition normalized to 10 $\mu$M navarixin response.

application of the assay to other GPCRs expressed by neutrophils. As FPR1 responses in neutrophil DMR assays have previously been characterized (Christensen et al., 2017), the FPR1 agonist fMLF was chosen as a positive control. A range of ligands were then tested, including those of classic neutrophil chemoattractant receptors such as the formyl peptide receptors (FPR1, FPR2, and FPR3), leukotriene $B_4$ receptors ($BLT_1$ and $BLT_2$), platelet activating factor (PAF) receptor, and complement component 5a receptor ($C5aR_1$), as well as other GPCRs that have been described as expressed on neutrophils, such as the free fatty acid receptor (FFAR) 2, and purinergic P2Y receptors (Le Poul et al., 2003; Futosi et al., 2013; Wang and Chen, 2018; Frei et al., 2021).

Responses to all ligands tested were detected and were shown to be reproducible and robust over multiple donors (Fig. 8; Table 7). All ligands exhibited a rapid initial peak within a few minutes of compound addition, similar to that observed with the CXCR1/CXCR2 chemokines, with some ligands, such as leukotriene $B_4$, showing a later secondary

peak (Fig. 8B), although for the purposes of analysis only the first peak was quantified. FPR responses were the largest in terms of wavelength change, with responses to both FPR1 and FPR2 selective ligands detected. As with the chemokine DMR studies, these assays demonstrated excellent signal to background (274 ± 123) and Z' (0.73 ± 0.03) when fMLF was used a positive control. Reassuringly, the potencies determined here for fMLF and CXCL8 match published results for neutrophil DMR (Locker et al., 2015; Christensen et al., 2017), further demonstrating the reproducibility of this assay across multiple laboratories.

## Discussion

Here we aimed to profile CXCR1 and CXCR2 responses in primary human neutrophils and validate neutrophil DMR as a higher throughput screening assay that could be used as an alternative to more conventional neutrophil functional assays, such as CD11b upregulation or chemotaxis for compound
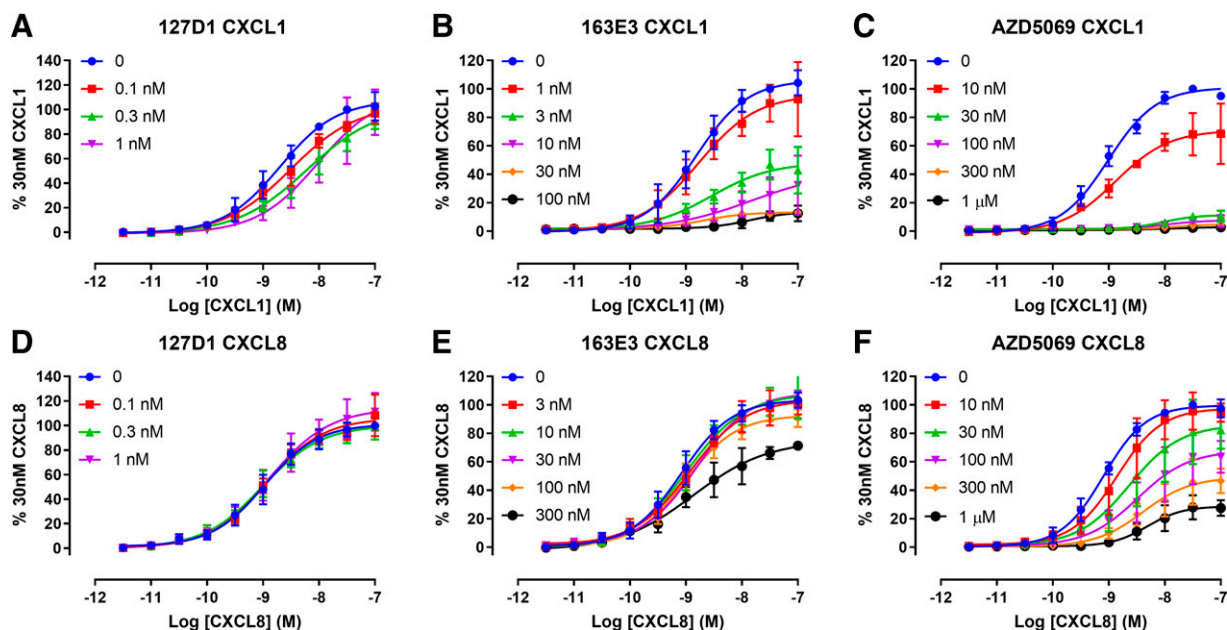


**Fig. 6.** Schild analysis AZD-5069 and CXCR2 nanobodies. Antagonists were preincubated with neutrophils for 1 hour at RT before addition of CXCL1 (A–C) or CXCL8 (D–F). Data are pooled (mean ± S.D.) of at least three independent experiments from individual donors performed in duplicate, normalized to vehicle treated 30 nM CXCL1 or 30 nM CXCL8 responses.
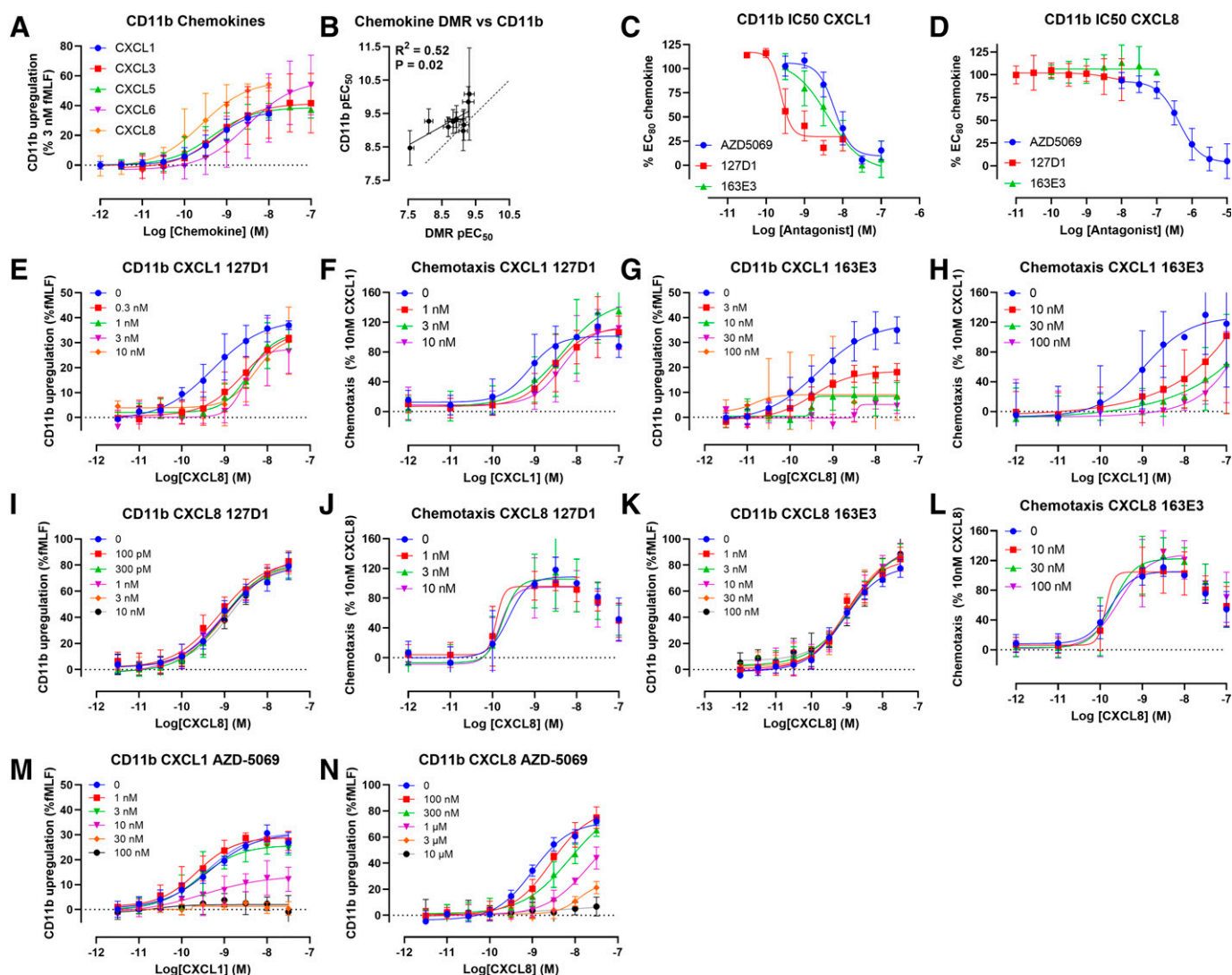
**Fig. 7.** Summary of CD11b and chemotaxis characterization data. CXCR1/2 chemokines induce upregulation of CD11b (A) with potencies correlating with potencies in the DMR assay (B). Antagonist activity (pIC$_{50}$) was determined by challenge of an EC$_{80}$ of CXCL1 (C) or CXCL8 (D) after preincubation of the antagonist for 30 minutes. CXCL1; Schild analysis of 127D1 in CD11b (E) and chemotaxis (F) assays and 163E3 in CD11b (G) and chemotaxis (H) assays. CXCL8; Schild analysis of 127D1 in CD11b (I) and chemotaxis (J) assays, and 163E3 in CD11b (K) and chemotaxis (L) assays. Schild analysis of AZD-5069 to inhibit CXCL1 (M) and CXCL8 (N) in CD11b assays. CD11b responses were normalized to 3 nM fMLF response and data are expressed as pooled (mean ± S.D) of three to nine independent donors. Chemotaxis responses were normalized to 10 nM chemokine response and data are expressed as pooled (mean ± S.D.) of four independent experiments from individual donors performed in quadruplicate. Data in the correlation plot is summarized from Table 6.

characterization. Neutrophils are of interest as a drug target for many indications (Bartneck and Wang, 2019; Cheng et al., 2019; Németh et al., 2020) so there is a need for higher throughput screening assays to determine compound activity at this cell type. However, the coexpression of closely related receptors can often confound results when moving from recombinant to primary cell systems. In neutrophils, the coexpression of CXCR1 and CXCR2 can lead to poor translation of compound effect across cell systems, with ligands that appear efficacious in cells overexpressing one receptor, losing either potency or efficacy, or both, for the inhibition of cross-reactive ligands. This was clearly demonstrated by the loss of CXCL8 inhibition in neutrophils by the CXCR2-specific nanobodies across all the neutrophil assay formats investigated, which was not observed or predicted from the CHO CXCR1 or CHO CXCR2 assays. Likewise, the significant increase in the concentrations of AZD-5069 required to inhibit neutrophil CXCL8

responses relative to CXCL1, despite having equal potency to inhibit both chemokines when tested in CHO CXCR2 cells, shows that this loss of translation is not just restricted to CXCR2-specific nanobodies. This was further highlighted by the reduced correlation for the antagonists between the recombinant data for the CXCL8-CXCR2 combination and neutrophil data, relative to CXCL1-CXCR2. This is likely due to the coactivation of CXCR1 by CXCL8, reducing the ability of the antagonists to fully block the chemokine signaling, due to the receptor redundancy in neutrophils allowing both CXCR1 and CXCR2 to signal. This further highlights the importance of the availability of a robust neutrophil screening assay.

Blockade of the CXCL8-CXCR2 interaction is postulated to be an effective strategy for cancer therapeutics given the wealth of evidence that CXCL8 drives tumor growth through immunosuppression, angiogenesis, and metastasis (David et al., 2016; Liu et al., 2016). The lack of CXCL8 inhibition by CXCR2-

TABLE 6
Summary of chemokine responses in neutrophil CD11b upregulation assays

| Chemokine | $pEC_{50}$ | $E_{max}$ (% 3 nM fMLF) | n |
|---|---|---|---|
| CXCL1 | $9.26 \pm 0.36$ | $35 \pm 8$ | 8 |
| CXCL2 | $9.27 \pm 0.19$ | $87 \pm 72$ | 4 |
| CXCL3 | $9.31 \pm 0.12$ | $43 \pm 16$ | 4 |
| CXCL5 | $9.16 \pm 0.21$ | $39 \pm 4$ | 5 |
| CXCL5 (5-78) | $8.98 \pm 0.27$ | $39 \pm 4$ | 5 |
| CXCL5 (9-78) | $9.85 \pm 0.21$ | $37 \pm 9$ | 5 |
| CXCL6 | $8.47 \pm 0.26$ | $55 \pm 14$ | 4 |
| CXCL7 | $10.08 \pm 0.69$ | $78 \pm 53$ | 4 |
| CXCL8 | $9.34 \pm 0.13$ | $70 \pm 22$ | 9 |
| CXCL8 (8-79) | $9.10 \pm 0.13$ | $58 \pm 8$ | 5 |

Data are expressed as pooled (mean ± S.D.) of at least four independent experiments from at least four individual donors, with maximal responses normalized to 3 nM fMLF response.

specific inhibitors in neutrophils, despite good inhibition in CHO CXCR2 assays, highlights the importance of testing ligands in disease-relevant primary cells. It also highlights that CXCR2-selective compounds may not be the most effective strategy for blocking CXCL8 signaling clinically and that dual blockade of CXCR1 and CXCR2 could be beneficial for significant blockade of neutrophil responses. This aspect has been particularly difficult to test in vivo as mice do not express a CXCL8 equivalent (David et al., 2016). While there are concerns that a dual blockade of CXCR1 and CXCR2 could lead to neutropenia, there is evidence that, in inflammatory conditions, where excessive immune cell infiltration is a key driver of disease, this dual blockade could be beneficial (Mattos et al., 2020). A recent report describing a CXCR2 antibody that fully blocks CXCL8-mediated chemotaxis in neutrophils (Shi et al., 2021) does suggest CXCR2-specific inhibitors could be efficacious in this respect; however, is likely that these inhibitors would require very specific receptor interactions. This is exemplified by the reported antibody possessing an almost overlapping epitope compared with the 127D1 nanobody (residues 13-16 for Shi et al. and 11, 14 and 15 for Bradley et al.; Bradley et al., 2015; Shi et al., 2021) and agrees with

studies that have demonstrated that a CXCR2-specific antibody is insufficient alone to inhibit higher concentrations of CXCL8 (Wu et al., 1996). As neutrophils express numerous structurally related GPCRs, for example, multiple formyl peptide receptors and leukotriene $B_4$ receptors (Futosi et al., 2013), it may be envisaged that these receptors may also suffer from issues in translation from recombinant screening systems to in vivo biology, where neutrophil screening assays could help to de-risk this.

While this study has concentrated on neutrophil responses, chemokine receptors are known to be expressed in different types of tumor cells, where they can modulate cell invasion, migration, and metastasis (Liu et al., 2019; Shang and Li, 2019). As a label-free technique, DMR can be used across a variety of cell types, including cancer cells (Du et al., 2009; Harris et al., 2017). While the effect of chemokines has not been looked at in cancer cells specifically, it could be interesting to understand whether this lack of translation for CXCR1/2 antagonists through from recombinant to native expressing cells is true of cancer cells as well as neutrophils.

Throughout the industry, there is a growing appreciation of the importance of primary cell screening to improve translation to the clinic, with approaches such as high content imaging and phenotypic screening being conducted on primary cells, disease-relevant induced pluripotent stem cells, or coculture models (Woo et al., 2019; Lin et al., 2020; Warchal et al., 2020). However, there is a need to balance cell accessibility and assay reproducibility against throughput. High content screening in particular can be time consuming, both in terms of the image acquisition and subsequent analysis (Lin et al., 2020). We believe DMR assays provide an important avenue to allow a medium throughput level of screening and, particularly when used with isolated blood cells, provide an easily accessible and reliable primary cell screen. The consistency of the antagonist profiles and level of inhibition across the different neutrophil assays gives us confidence that the DMR assay is predictive of CD11b and chemotaxis responses, both assays that are thought to be more mechanistically linked to disease pathologies but generally suffer from low throughput and variability.
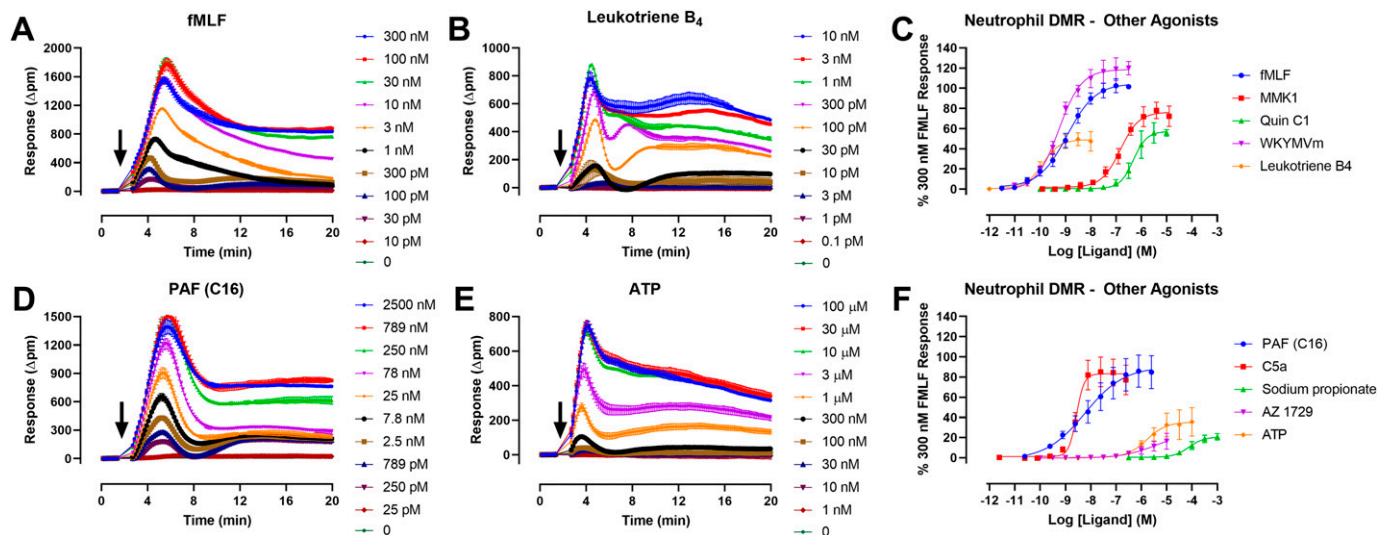
**Fig. 8.** Neutrophil DMR responses to GPCR ligands. Representative example kinetic traces of GPCR ligands fMLF (A), leukotriene $B_4$ (B), PAF (C16) (D), and ATP (E) with arrow indicating compound addition. Data points represent mean ± S.D. of duplicate wells. Data were baseline corrected and peak responses between 3 and 7 minutes were extracted (C, F). Data shown are pooled (mean ± S.D.) of three to six independent experiments from individual donors performed in duplicate.

TABLE 7
Summary of GPCR ligand responses in neutrophil DMR assays

| Receptor | Ligand | $pEC_{50}$ | $E_{max}$ (% 300 nM fMLF) | n |
|---|---|---|---|---|
| FPR1 / FPR2 | fMLF | $8.93 \pm 0.16$ | $106 \pm 7$ | 6 |
| FPR2 | MMK1 | $6.84 \pm 0.10$ | $75 \pm 9$ | 6 |
| FPR2 | Quin C1 | $6.27 \pm 0.14$ | $59 \pm 4$ | 3 |
| FPR1 / FPR2 / FPR3 | WKYMVm | $9.27 \pm 0.08$ | $119 \pm 8$ | 3 |
| $BLT_1$ / $BLT_2$ | Leukotriene $B_4$ | $9.88 \pm 0.23$ | $50 \pm 9$ | 5 |
| PAF receptor | PAF (C16) | $8.23 \pm 0.26$ | $90 \pm 15$ | 6 |
| $C5aR_1$ | C5a | $8.56 \pm 0.06$ | $83 \pm 12$ | 5 |
| FFAR2 / FFAR3 | Sodium propionate | $4.13 \pm 0.16$ | $21 \pm 2$ | 5 |
| FFAR2 | AZ 1729 | $5.50 \pm 0.19$ | $25 \pm 11$ | 3 |
| P2Y | ATP | $5.83 \pm 0.24$ | $36 \pm 12$ | 3 |

$C5aR_1$, complement component 5a receptor 1; FFA, free fatty acid; PAF, platelet activating factor.
Data are pooled (mean ± S.D.) of at least three independent experiments performed in duplicate, with data normalized to 300 nM fMLF response.

Furthermore, the ability to detect a wide range of GPCR responses exemplifies the utility of this assay beyond the chemokine receptors initially profiled. As CD11b upregulation has been used as a target engagement marker in clinical studies of free fatty acid receptor 2, $BLT_1$, and complement component 5a receptor 1 ligands (Liston et al., 1998; Bekker et al., 2016; Namour et al., 2016), profiling ligands in the DMR assay could allow higher throughput compound characterization in an assay platform that may provide increased confidence of success through to the clinic.

Finally, despite the current dogma that only CXCL6 and CXCL8 are ligands for CXCR1 (Ahuja and Murphy, 1996; Liu et al., 2016), the data generated here show that all the chemokines studied will activate CXCR1 at the concentrations examined, except for CXCL2, which was CXCR2 specific at up 200 nM. However, all chemokines were selective for CXCR2, except for the CXCL8 proteoforms, which were equipotent across both receptors. Interestingly, a truncated form of CXCL5 [CXCL5 (9-78)], which occurs naturally in vivo (Nufer et al., 1999; Mortier et al., 2008), was surprisingly more potent at CXCR1 than the well-documented high affinity CXCR1 ligand CXCL6 (Table 1), suggesting that the role of CXCR1 in CXCL5 effects in disease should be considered in the future.

In summary, we present the neutrophil DMR assay as a medium throughput alternative to established neutrophil functional assays, such as chemotaxis and CD11b. The correlation with CD11b upregulation assays is of particular significance given their prevalence as target engagement markers in early clinical studies; this translation gives confidence that a compound will maintain its activity in vivo and thereby increase the likelihood of progressing to the clinic. DMR assays are robust, are reproducible, yield high-quality data that is compatible with industry screening standards, and are predictive of activity in other neutrophil assays. We have demonstrated that these neutrophil DMR assays are highly effective in supporting the study of the chemokine receptors CXCR1 and CXCR2 and that these assays could be more broadly applied to other GPCRs expressed on neutrophils.

### Acknowledgments

### Data Availability

The authors declare that all the data supporting the findings of this study are available within the paper and its Supplemental Material.

### Authorship Contributions

### References

Ahuja SK and Murphy PM (1996) The CXC chemokines growth-regulated oncogene (GRO) α, GRObeta, GROgamma, neutrophil-activating peptide-2, and epithelial cell-derived neutrophil-activating peptide-78 are potent agonists for the type B, but not the type A, human interleukin-8 receptor. *J Biol Chem* **271**:20545–20550.

Bartneck M and Wang J (2019) Therapeutic targeting of neutrophil granulocytes in inflammatory liver disease. *Front Immunol* **10**:2257.

Bekker P, Dairaghi D, Seitz L, Leleti M, Wang Y, Ertl L, Baumgart T, Shugarts S, Lohr L, Dang T et al. (2016) Characterization of pharmacologic and pharmacokinetic properties of CCX168, a potent and selective orally administered complement 5a receptor inhibitor, based on preclinical evaluation and randomized phase 1 clinical study. *PLoS One* **11**:e0164646.

Bertini R, Allegretti M, Bizzarri C, Moriconi A, Locati M, Zampella G, Cervellera MN, Di Cioccio V, Cesta MC, Galliera E et al. (2004) Noncompetitive allosteric inhibitors of the inflammatory chemokine receptors CXCR1 and CXCR2: prevention of reperfusion injury. *Proc Natl Acad Sci USA* **101**:11791–11796.

Bradley ME, Bond ME, Manini J, Brown Z, and Charlton SJ (2009) SB265610 is an allosteric, inverse agonist at the human CXCR2 receptor. *Br J Pharmacol* **158**:328–338.

Bradley ME, Dombrecht B, Manini J, Willis J, Vlerick D, De Taeye S, Van den Heede K, Roobrouck A, Grot E, Kent TC et al. (2015) Potent and efficacious inhibition of CXCR2 signaling by biparatopic nanobodies combining two distinct modes of action. *Mol Pharmacol* **87**:251–262.

Cheng Y, Ma X, Wei Y, and Wei X-W (2019) Potential roles and targeted therapy of the CXCLs/CXCR2 axis in cancer and inflammatory diseases. *Biochimica Biophysica Acta - Rev Cancer* **1871**:289–312.

Christensen HB, Gloriam DE, Pedersen DS, Cowland JB, Borregaard N, and Bräuner-Osborne H (2017) Applying label-free dynamic mass redistribution assay for studying endogenous FPR1 receptor signalling in human neutrophils. *J Pharmacol Toxicol Methods* **88**:72–78.

David JM, Dominguez C, Hamilton DH, and Palena C (2016) The IL-8/IL-8R axis: a double agent in tumor immune resistance. *Vaccines (Basel)* **4**:22.

Du Y, Li Z, Li L, Chen ZG, Sun SY, Chen P, Shin DM, Khuri FR, and Fu H (2009) Distinct growth factor-induced dynamic mass redistribution (DMR) profiles for monitoring oncogenic signaling pathways in various cancer cells. *J Recept Signal Transduct Res* **29**:182–194.

Dwyer MP, Yu Y, Chao J, Aki C, Chao J, Biju P, Girijavallabhan V, Rindgen D, Bond R, Mayer-Ezel R et al. (2006) Discovery of 2-hydroxy-N,N-dimethyl-3-2-[[(R)-1-(5- methyl-furan-2-yl)propyl]amino]-3,4-dioxocyclobut-1-enylaminobenzamide (SCH 527123): a potent, orally bioavailable CXCR2/CXCR1 receptor antagonist. *J Med Chem* **49**:7603–7606.

Dyer DP (2020) Understanding the mechanisms that facilitate specificity, not redundancy, of chemokine-mediated leukocyte recruitment. *Immunology* **160**:336–344.

Eglen RM, Gilchrist A, and Reisine T (2008) The use of immortalized cell lines in GPCR screening: the good, bad and ugly. *Comb Chem High Throughput Screen* **11**:560–565.

Fang Y (2011) Label-free receptor assays. *Drug Discov Today Technol* **7**:e5–e11.

Frei R, Nordlohne J, Hüser U, Hild S, Schmidt J, Eitner F, and Grundmann M (2021) Allosteric targeting of the FFA2 receptor (GPR43) restores responsiveness of desensitized human neutrophils. *J Leukoc Biol* **109**:741–751.

Futosi K, Fodor S, and Mócsai A (2013) Neutrophil cell surface receptors and their intracellular signal transduction pathways. *Int Immunopharmacol* **17**:638–650.

Gomez-Lopez N, Vadillo-Ortega F, and Estrada-Gutierrez G (2011) Combined boyden-flow cytometry assay improves quantification and phenotypification of leukocyte chemotaxis. *PLoS One* **6**:e28771.

Grundmann M and Kostenis E (2015) Label-free biosensor assays in GPCR screening. *Methods Mol Biol* **1272**:199–213.

Harris D-A, Park J-M, Soon-Lee K, Xu C, Stella N, and Hague C (2017) Label-free dynamic mass redistribution reveals low density, pro-survival α1B-adrenergic receptors in human SW480 colon carcinoma cells. *J Pharmacol Exp Ther* **361**:219–228.

Hillger JM, Lieuw W-L, Heitman LH, and IJzerman AP (2017) Label-free technology and patient cells: from early drug development to precision medicine. *Drug Discov Today* **22**:1808–1815.

Lämmermann T and Kastenmüller W (2019) Concepts of GPCR-controlled navigation in the immune system. *Immunol Rev* **289**:205–231.

Lazaar AL, Sweeney LE, MacDonald AJ, Alexis NE, Chen C, and Tal-Singer R (2011) SB-656933, a novel CXCR2 selective antagonist, inhibits ex vivo neutrophil activation and ozone-induced airway inflammation in humans. *Br J Clin Pharmacol* **72**:282–293.

Lin S, Schorpp K, Rothenaigner I, and Hadian K (2020) Image-based high-content screening in drug discovery. *Drug Discov Today* **25**:1348–1361.

Liston TE, Conklyn MJ, Houser J, Wilner KD, Johnson A, Apseloff G, Whitacre C, and Showell HJ (1998) Pharmacokinetics and pharmacodynamics of the leukotriene B4 receptor antagonist CP-105,696 in man following single oral administration. *Br J Clin Pharmacol* **45**:115–121.

Liu G, An L, Zhang H, Du P, and Sheng Y (2019) Activation of CXCL6/CXCR1/2 axis promotes the growth and metastasis of osteosarcoma cells *in vitro* and *in vivo*. *Front Pharmacol* **10**:307.

Liu K, Wu L, Yuan S, Wu M, Xu Y, Sun Q, Li S, Zhao S, Hua T, and Liu Z-J (2020) Structural basis of CXC chemokine receptor 2 activation and signalling. *Nature* **585**:135–140.

Liu Q, Li A, Tian Y, Wu JD, Liu Y, Li T, Chen Y, Han X, and Wu K (2016) The CXCL8-CXCR1/2 pathways in cancer. *Cytokine Growth Factor Rev* **31**:61–71.

Locker F, Lang AA, Koller A, Lang R, Bianchini R, and Kofler B (2015) Galanin modulates human and murine neutrophil activation in vitro. *Acta Physiol (Oxf)* **213**:595–602.

Maas SL, Soehnlein O, and Viola JR (2018) Organ-specific mechanisms of transendothelial neutrophil migration in the lung, liver, kidney, and aorta. *Front Immunol* **9**:2739.

Mattos MS, Ferrero MR, Kraemer L, Lopes GAO, Reis DC, Cassali GD, Oliveira FMS, Brandolini L, Allegretti M, Garcia CC et al. (2020) CXCR1 and CXCR2 inhibition by ladarixin improves neutrophil-dependent airway inflammation in mice. *Front Immunol* **11**:566953.

McCracken JM, and Allen L-AH (2014) Regulation of human neutrophil apoptosis and lifespan in health and disease. *J Cell Death* **7**:15–23.

Miller BE, Mistry S, Smart K, Connolly P, Carpenter DC, Cooray H, Bloomer JC, Tal-Singer R, and Lazaar AL (2015) The pharmacokinetics and pharmacodynamics of danirixin (GSK1325756)— a selective CXCR2 antagonist —in healthy adult subjects. *BMC Pharmacol Toxicol* **16**:18.

Mortier A, Van Damme J, and Proost P (2008) Regulation of chemokine activity by posttranslational modification. *Pharmacol Ther* **120**:197–217.

Namour F, Galien R, Van Kaem T, Van der Aa A, Vanhoutte F, Beetens J, and Van't Klooster G (2016) Safety, pharmacokinetics and pharmacodynamics of GLPG0974, a potent and selective FFA2 antagonist, in healthy male subjects. *Br J Clin Pharmacol* **82**:139–148.

Németh T, Sperandio M, and Mócsai A (2020) Neutrophils as emerging therapeutic targets. *Nat Rev Drug Discov* **19**:253–275.

Nicholls DJ, Wiley K, Dainty I, MacIntosh F, Phillips C, Gaw A, and Mårdh CK (2015) Pharmacological characterization of AZD5069, a slowly reversible CXC chemokine receptor 2 antagonist. *J Pharmacol Exp Ther* **353**:340–350.

Nufer O, Corbett M, and Walz A (1999) Amino-terminal processing of chemokine ENA-78 regulates biological activity. *Biochemistry* **38**:636–642.

Le Poul E, Loison C, Struyf S, Springael J-Y, Lannoy V, Decobecq M-E, Brezillon S, Dupriez V, Vassart G, Van Damme J et al. (2003) Functional characterization of human receptors for short chain fatty acids and their role in polymorphonuclear cell activation. *J Biol Chem* **278**:25481–25489.

Salchow K, Bond ME, Evans SC, Press NJ, Charlton SJ, Hunt PA, and Bradley ME (2010) A common intracellular allosteric binding site for antagonists of the CXCR2 receptor. *Br J Pharmacol* **159**:1429–1439.

Schröder R, Schmidt J, Blättermann S, Peters L, Janssen N, Grundmann M, Seemann W, Kaufel D, Merten N, Drewke C et al. (2011) Applying label-free dynamic mass redistribution technology to frame signaling of G protein-coupled receptors noninvasively in living cells. *Nat Protoc* **6**:1748–1760.

Scott CW and Peters MF (2010) Label-free whole-cell assays: expanding the scope of GPCR screening. *Drug Discov Today* **15**:704–716.

Shang FM and Li J (2019) A small-molecule antagonist of CXCR1 and CXCR2 inhibits cell proliferation, migration and invasion in melanoma via PI3K/AKT pathway. *Med Clin (Barc)* **152**:425–430.

Shi X, Wan Y, Wang N, Xiang J, Wang T, Yang X, Wang J, Dong X, Dong L, Yan L et al. (2021) Selection of a picomolar antibody that targets CXCR2-mediated neutrophil activation and alleviates EAE symptoms. *Nat Commun* **12**:2547.

Silvestre-Roig C, Fridlender ZG, Glogauer M, and Scapini P (2019) Neutrophil diversity in health and disease. *Trends Immunol* **40**:565–583.

Stott LA, Hall DA, and Holliday ND (2016) Unravelling intrinsic efficacy and ligand bias at G protein coupled receptors: a practical guide to assessing functional data. *Biochem Pharmacol* **101**:1–12.

Wang X and Chen D (2018) Purinergic regulation of neutrophil function. *Front Immunol* **9**:399.

Warchal SJ, Dawson JC, Shepherd E, Munro AF, Hughes RE, Makda A, and Carragher NO (2020) High content phenotypic screening identifies serotonin receptor modulators with selective activity upon breast cancer cell cycle and cytokine signaling pathways. *Bioorg Med Chem* **28**:115209.

Woo LA, Tkachenko S, Ding M, Plowright AT, Engkvist O, Andersson H, Drowley L, Barrett I, Firth M, Akerblad P et al. (2019) High-content phenotypic assay for proliferation of human iPSC-derived cardiomyocytes identifies L-type calcium channels as targets. *J Mol Cell Cardiol* **127**:204–214.

Wu L, Ruffing N, Shi X, Newman W, Soler D, Mackay CR, and Qin S (1996) Discrete steps in binding and signaling of interleukin-8 with its receptor. *J Biol Chem* **271**:31202–31209.

**Address correspondence to:** Dr. Lisa A. Stott, Sosei Heptares, Steinmetz Building, Granta Park, Cambridge, CB21 6DG, United Kingdom. E-mail: lisa.stott@soseiheptares.com

The Journal of Pharmacology and Experimental Therapeutics

JPET-AR-2023-001787

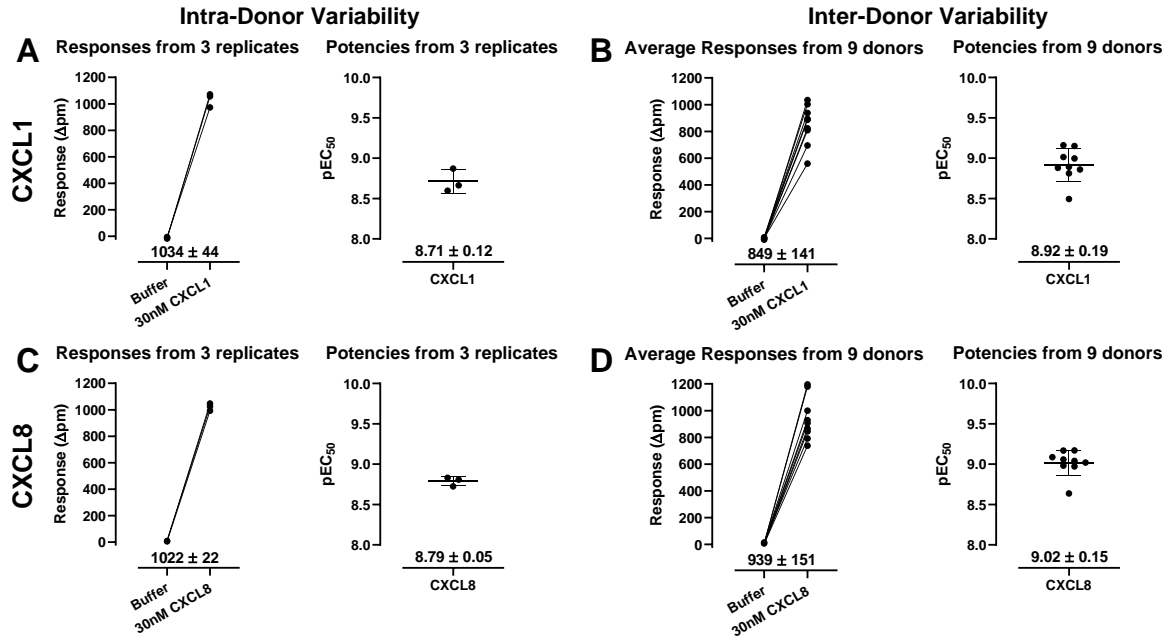**Supplemental Material**

**The neutrophil dynamic mass redistribution assay as a medium throughput primary cell screening assay**

Lisa A. Stott, Armand Drieu la Rochelle, Susan Brown, Greg Osborne, Catherine J. Hutchings, Simon Poulter, Kirstie A. Bennett, Matt Barnes

LAS, ADR, SB, GO, SP, KB, MB: Sosei Heptares, Cambridge

CJH: Independent Consultant

## Intra-Donor Variability

**A**  Responses from 3 replicates   Potencies from 3 replicates

CXCL1

1034 ± 44

Buffer 30nM CXCL1

8.71 ± 0.12

CXCL1

**C**  Responses from 3 replicates   Potencies from 3 replicates

CXCL8

1022 ± 22

Buffer 30nM CXCL8

8.79 ± 0.05

CXCL8

## Inter-Donor Variability

**B**  Average Responses from 9 donors   Potencies from 9 donors

849 ± 141

Buffer 30nM CXCL1

8.92 ± 0.19

CXCL1

**D**  Average Responses from 9 donors   Potencies from 9 donors

939 ± 151

Buffer 30nM CXCL8

9.02 ± 0.15

CXCL8

**Supplemental Figure 1: Intra- and inter-donor variability in response size and potency.**

Variability of CXCL1 response size and potency between experimental replicates (A) and across multiple donors (B). Variability of CXCL8 response size and potency between experimental replicates (C) and across multiple donors (D).
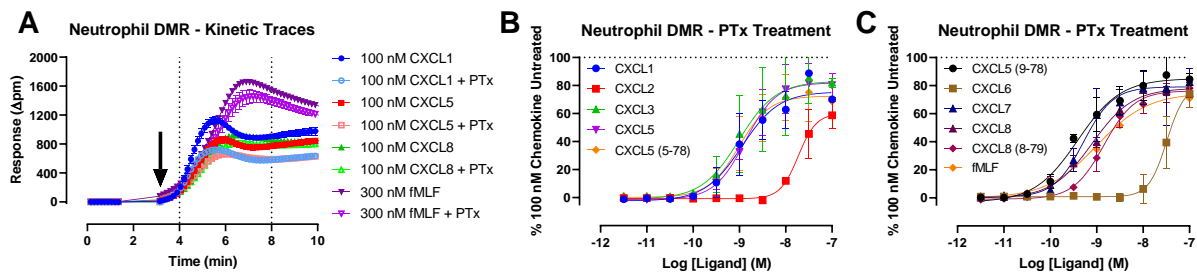


**Supplemental Figure 2: Pertussis toxin partially inhibits neutrophil chemokine and fMLF responses.** Representative kinetic DMR traces for 100 nM CXCL1, CXCL5 and CXCL8, and 300 nM fMLF with and without 1 h 3 μg ml$^{-1}$ pertussis toxin (PTx) treatment at 37°C (A). Data points represent mean ± SD of triplicate wells. Following PTx pre-treatment, cells were seeded for 2 h at RT before stimulating with chemokine according to the standard protocol. Data were baseline corrected by subtracting buffer wells and peak response between 4-8 min extracted and plotted, normalised to

each individual chemokine response at 100 nM in the absence of PTx pre-treatment (B, C). Data

represent pooled (mean ± SD) of 2 independent experiments from 2 individual donors.
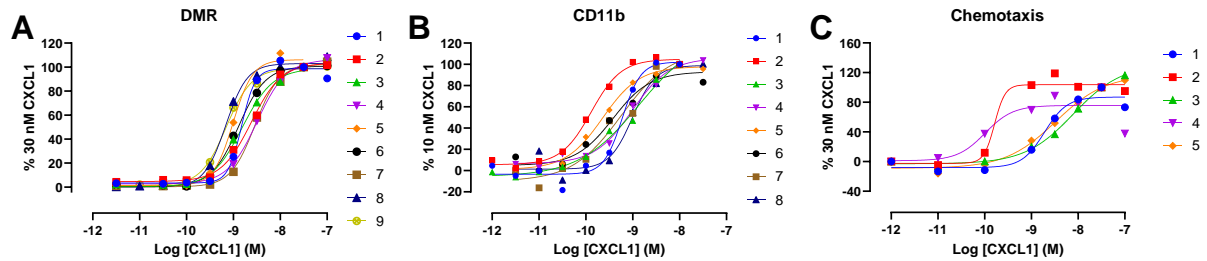


**Supplemental Figure 3**: **Inter-donor variability of neutrophil assays.** Example CXCL1

concentration response curves for individual donors in DMR (A), CD11b (B) and chemotaxis

assays (C). Each data point represents mean value from 2-4 replicates, normalized to maximal

CXCL1 response.